The following pages of this pdf are from the page proofs. Unfortunately, I do not have the pdf of the final version. The page proofs contain a few typesetting errors (b instead of β etc.). However the chapter number in the book is chapter 2 not chapter 6 and the page range is 27-56, not 111-140.

6

Folding and Stability of Monomeric β-Barrel Membrane Proteins

Jörg H. Kleinschmidt

6.1
Introduction

Integral membrane proteins fall into two different classes that can be distinguished by their transmembrane secondary structure: α-helical and β-barrel proteins. Within the hydrophobic core of the membrane, all hydrogen-bonding donors and acceptors of the polypeptide backbone form hydrogen bonds. The nonpolar side-chains face the hydrophobic acyl chains of the membrane lipids. While the more abundant α-helical transmembrane proteins are found in the cytoplasmic (or inner) membranes, the integral membrane proteins with β-barrel structures are known from outer membranes of bacteria, mitochondria and chloroplasts. The β-barrel is characterized by the number of antiparallel β-strands and by the shear number, which is a measure for the inclination angle of the β-strands against the barrel axis. The outer membrane proteins (OMPs) of bacteria form transmembrane β-barrels with even numbers of β-strands ranging from eight to 22 with shear numbers from 8 to 24 [1]. The strands are tilted by 36–44° relative to the barrel axis [1, 2]. Examples are OmpA [3, 4], OmpX [5–7], NspA [8], and PagP [9, 10] (eight β-strands); OmpT [11] (10 β-strands); NalP [12] and OmPlA [13] (12 β-strands); FadL [14] (14 β-strands); Omp32 [15], matrix porin [16], OmpF [17] and PhoE [18] (16 β-strands); maltoporin (LamB) [19] and sucrose porin (ScrY) [20] (18 β-strands); and FepA [21], BtuB [22, 23] and FhuA [24, 25] (22 β-strands). Monomers (OmpA, FhuA and OmpG [26]), dimers (OmPlA) and trimers (OmpF and PhoE) are known. The β-barrel membrane proteins serve a wide range of different functions. They can be non-specific diffusion pores (OmpA, OmpC and OmpF), specific pores (LamB and ScrY), active transporters (FhuA, FepA and BtuB), enzymes such as proteases (OmpT), lipases (OmPlA), acyltransferases (PagP) or, like TolC, involved in solute efflux [27]. Some examples of β-barrel membrane proteins are shown in Fig. 6.1. Recently developed screening algorithms for the genomic identification of β-barrel
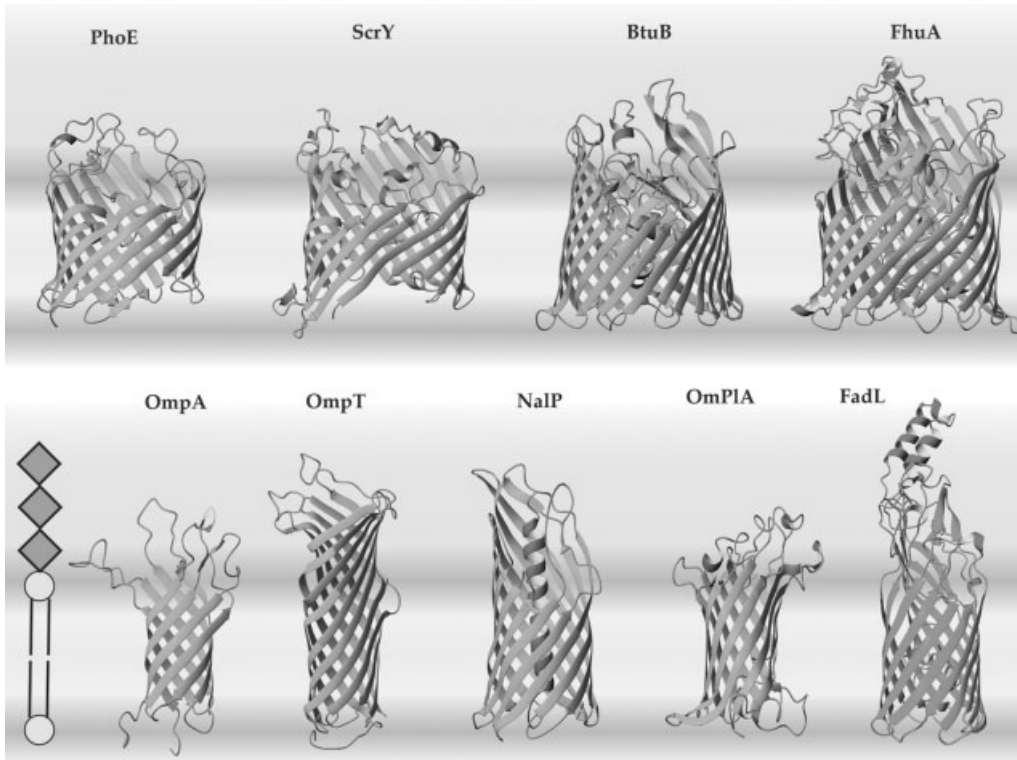
Fig. 6.1 Some representative crystal structures of β-barrel membrane proteins of the outer membranes of bacteria are shown. Transmembrane β-barrels have an even number of antiparallel transmembrane strands, which is eight for OmpA (shown here is the nuclear magnetic resonance structure from [3]; for the crystal structure, see [4, 94]), 10 for OmpT [11], 12 for NalP [12] and OmPlA [13], 14 for FadL [14], 16 for PhoE [18], 18 for ScrY [11], and 22 for BtuB [22] and FhuA [24]. OmpA is a small ion channel [73], OmpT is a protease, NalP is an autotransporter, FadL is a long-chain fatty acid transporter, PhoE is a diffusion pore, ScrY is a sucrose-specific porin and OmPlA is a phospholipase. BtuB and FhuA are active transporters for ferrichrome iron and vitamin B_{12} uptake, respectively. OMPs of mitochondria are predicted to form similar transmembrane β-barrels. Examples are the voltage-dependent anion channels, out of which more than a dozen have been sequenced [144]. Protein structures were generated with MolMol [145].

membrane proteins indicate that there are many still not characterized OMPs, e.g. in the genomes of *Escherichia coli* and *Pseudomonas aeruginosa* [28, 29]. Soluble bacterial toxins that can insert into membranes, such as α-hemolysine from *Staphylococcus aureus* [30] and perfringolysine O from *Clostridium perfringens* [31, 32], also form β-barrels, but these are oligomeric. This chapter focuses on the stability and folding of monomeric β-barrels from bacteria. For reviews on the membrane insertion and assembly of pore forming toxins, see, e.g. [33–35]. For

a review on the oligmeric *β*-barrels from mycobacteria, such as MspA from *Mycobacterium smegmatis* [36], see, e.g. [37].

6.2
Stability of *β*-Barrel Membrane Proteins

Since most membrane proteins have a high thermal stability and are difficult to unfold in solution [38], it is not easy to experimentally determine the free energy of membrane insertion and folding of integral membrane proteins, which is equivalent to the free energy of unfolding from the membrane. Exceptions have been the *β*-barrel membrane proteins, which are generally characterized by a relatively low average hydrophobicity and can therefore be completely solubilized in concentrated solutions of a chemical denaturant, e.g. urea. The thermodynamic stability of the ferric enterobactin receptor (FepA) was studied after solubilization of FepA in detergent micelles and a recent study on the stability of OmpA in lipid bilayers indicated that bilayer properties strongly influence the stability of integral membrane proteins.

6.2.1
Thermodynamic Stability of FepA in Detergent Micelles

The first report on the thermodynamic stability of integral *β*-barrel membrane proteins by equilibrium unfolding experiments came from Feix et al. [39], who determined the free energy of unfolding of FepA in Triton X-100 detergent micelles. Unfolding was induced with increasing concentrations of urea or, alternatively, of guanidinium chloride as chemical denaturants. The linearity of the dependence of unfolding equilibria on the denaturant concentration has been demonstrated many times for soluble proteins [40–43] and was confirmed for FepA unfolding from Triton X-100 detergent micelles [39] and later for OmpA from phospholipid bilayers [44]. The free energy of unfolding in absence of denaturant, $\Delta G_U^0(H_2O)$, could therefore be extrapolated from the free energies of unfolding in presence of different concentrations of denaturant, ΔG_U^0 ([denaturant]), according to

$$\Delta G_U^0(H_2O) = \Delta G_U^0([\text{denaturant}]) + m \cdot [\text{denaturant}]$$

where the *m* value is independent of the denaturant concentration, but a specific parameter that depends on the protein, the denaturant, the solvents (aqueous solutions of soluble proteins, solutions of detergent micelle/membrane protein complexes or solutions of membrane proteins in lipid vesicles) and on other parameters, such as temperature and pH. The *m* value can be linked to the increase of the denaturant exposed surface upon protein unfolding and is also a measure for the cooperativity of unfolding [45, 46]. Using site-directed spin-labeling (SDSL) electron spin resonance (ESR) spectroscopy, Klug et al. [39] reported a free energy $\Delta G_U^0(H_2O) = 6.05 \pm 0.6 \text{ kcal mol}^{-1}$ at 22 °C and pH 7.2 for

unfolding of FepA from Triton X-100 detergent micelles with an equilibrium transition midpoint at 5.5 M urea and an *m*-value of 1.1 ± 0.1 kcal mol^{-1} M^{-1}. They obtained a similar value, $\Delta G_U^0(H_2O) = 6.4$ kcal mol^{-1}, when unfolding was performed using guanidinium chloride (GdnHCl), but with a transition mid-point at 2.0 ± 0.1 M GdnHCl and an *m*-value of 3.3 ± 0.1 kcal mol^{-1} M^{-1}. The free energy of unfolding of FepA from Triton X-100 corresponded well with the free energies of unfolding of many water-soluble globular proteins, such as myoglobin, lysozyme, ribonuclease or barnase, which all have $\Delta G_U^0(H_2O)$ values in the range of 5–10 kcal mol^{-1} [42, 43, 47, 48].

Using SDSL ESR spectroscopy, the local stabilities of FepA along the fourth transmembrane *β*-strand (residues 244–256) were determined at pH 7 and at room temperature after solubilizing FepA in 2% Triton X-100 [49]. The stability of the *β*-strand and the cooperativity of unfolding were maximal for amino acid residues near the center of the *β*-strand at residue 250. A single-site cysteine mutant that was spin-labeled at this position and ESR spectroscopy were used to determine a stability of $\Delta G_U^0(H_2O) = 9.4$ kcal mol^{-1} ($m = 5.8$ kcal mol^{-1} M^{-1}) at this location in FepA. When determined for additionally prepared single-site cysteine mutants, the stability of the *β*-strand decreased from residue 250 towards residue 244 $[\Delta G_U^0(H_2O) = 7.1$ kcal mol^{-1}, $m = 3.3$ kcal mol^{-1} M$^{-1}]$ and towards residue 256 $[\Delta G_U^0(H_2O) = 2.4$ kcal mol^{-1}, $m = 1.3$ kcal mol^{-1} M$^{-1}]$, respectively [49].

6.2.2
Thermodynamic Stability of OmpA in Phospholipids Bilayers

First experimental data on the thermodynamic stability of an integral membrane protein in lipid bilayers was presented recently by Hong and Tamm [44] for OmpA. Since OmpA folds quantitatively at pH 10 from a fully denatured state in 8 M urea upon dilution of the denaturant in the presence of preformed lipid bilayers of phosphatidylcholine [50, 51] or mixtures of phosphatidylcholine and phosphatidylglycerol [52], Hong and Tamm studied the equilibrium unfolding of OmpA from model membranes using intrinsic fluorescence spectroscopy. Un-folding/folding equilibria were studied at 37.5 °C, i.e. above the gel-to-liquid-crystalline phase transition temperature of the phospholipids and with small unila-mellar vesicles (SUVs) prepared by ultrasonication. It was found that the free energy of unfolding of OmpA from lipid bilayers depends on the length of the fatty acyl chains and on the headgroup of the phospholipid. In a reference bilayer, composed of 92.5% palmitoyloleoylphosphatidylcholine ($C_{16:0}C_{18:1}$PC) and 7.5% pal-mitoyloleoylphosphatidylglycerol ($C_{16:0}C_{18:1}$PG) the free energy of unfolding was $\Delta G_U^0(H_2O) = 3.4$ kcal mol^{-1} (pH 10, 37.5 °C, $m = 1.1$ kcal mol^{-1} M^{-1}). The study nicely demonstrated the large dependence of the thermodynamic stability of OmpA on the composition of the lipid bilayer and on the chemical structure of the lipids, highlighting the important role of membrane phospholipids in the stabilization of integral membrane proteins. Based on the reference bilayer, the effects of the lipid chain length, degree of unsaturation of the acyl chains and lipid headgroup were investigated by varying the content of such a phospholipid at the

expense of $C_{16:0}C_{18:1}$PC and at constant 7.5% $C_{16:0}C_{18:1}$PG in this lipid bilayer. The stability $\Delta G^0_U(H_2O)$ of OmpA decreased with decreasing chain length of the phospholipids upon incorporation of increasing percentages of short-chain lipids (diC$_{10:0}$PC to diC$_{14:0}$PC). When phospholipids with longer acyl chains (e.g. $C_{18:0}C_{18:1}$PC) were incorporated, the stability of OmpA increased with increasing amounts of $C_{18:0}C_{18:1}$PC. An even stronger stability increase was observed, when the phosphatidylcholine lipid $C_{16:0}C_{18:1}$PC was replaced by the corresponding phosphatidylethanolamine ($C_{16:0}C_{18:1}$PE). For example, the free energies of OmpA unfolding from membranes composed of 7.5% $C_{16:0}C_{18:1}$PG and 62.5% $C_{16:0}C_{18:1}$PC host lipids and 30% of guest lipid were $\Delta G^0_U(H_2O) = 5.0$ kcal mol^{-1} with $C_{16:0}C_{18:1}$PE, $\Delta G^0_U(H_2O) = 3.9$ kcal mol^{-1} with $C_{18:0}C_{18:1}$PC, $\Delta G^0_U(H_2O) = 2.9$ kcal mol^{-1} with diC$_{12:0}$PC or diC$_{14:0}$PC and $\Delta G^0_U(H_2O) = 2.2$ kcal mol^{-1} with diC$_{10:0}$PC. For each lipid species, the dependence of $\Delta G^0_U(H_2O)$ on the concentration of this lipid appeared to be linear, when increased at the expense of $C_{16:0}C_{18:1}$PC in bilayers containing a constant amount of 7.5% of $C_{16:0}C_{18:1}$PG. Surprisingly, when lipids with two unsaturated acyl chains were incorporated into the reference bilayer, values for $\Delta G^0_U(H_2O)$ increased with decreasing length of the fatty acyl chains, reversing the effect seen for saturated and mono-unsaturated lipids. Two unsaturated acyl chains in a diacylphospholipid induce smaller elastic moduli and larger curvature stresses in lipid bilayers [53], which might explain these observations.

6.2.3
Thermal Stability of FhuA in Detergent Micelles

The thermal stability of ferric hydroxamate uptake protein A (FhuA) in *N,N*-dimethyl-*N*-lauryl amine *N*-oxide (LDAO) detergent micelles was recently studied by Bonhivers et al. [54]. FhuA showed two unfolding maxima in differential scanning calorimetry. In the absence of the ferrichrome iron ligand, wild-type (wt)-FhuA unfolding maxima were at $T_1 = 65\,°C$ and at $T_2 = 74.4\,°C$ with corresponding enthalpies of 140 and 160 kcal mol^{-1} [54], suggesting that there are two autonomous folding units in FhuA. In presence of ferrichrome iron, the first transition was shifted up to 71.4 °C, while T_2 remained constant. A mutant form, FhuAΔ21–128, in which a large part of the N-terminal cork domain was removed, showed only one transition at 62 °C and an enthalpy of 200 kcal mol^{-1}, independent of the presence of ferrichrome iron. This indicated that ferrichrome iron stabilized the cork domain and that the cork domain stabilized the 22-stranded β-barrel. However, reversibility of unfolding was not investigated and free energies of unfolding were not determined. Klug et al. had previously found that ferric enterobactin has limited stability at room temperature and, therefore, they could not compare the effect of this ligand on the thermodynamic stability of FepA. However, they also reported that the unfolding kinetics of FepA were slower in presence of ferric enterobactin [39], indicating a stabilizing effect of ferric enterobactin on FepA, which is consistent with the effect of ferrichrome iron on the denaturation temperature of FhuA [54].

6.3
Insertion and Folding of Transmembrane *b*-Barrel Proteins

6.3.1
Insertion and Folding of *b*-Barrel Membrane Proteins in Micelles

First *in vitro* refolding studies of integral membrane proteins were performed by Henning et al. in 1978 and demonstrated that the eight-stranded β-barrel OmpA develops native structure when incubated with lipopolysaccharide (LPS) and Triton X-100 after dilution of the denaturants sodium dodecylsulfate (SDS) or urea [55]. Similarly, Dornmair et al. [56] showed that after heat-induced unfolding in SDS micelles, OmpA refolds into micelles of the detergent octylglucoside even in the absence of LPS. These results on the β-barrel OmpA, and the successful refolding of bacteriorhodopsin that consists of a bundle of seven transmembrane α-helices and was first refolded by Khorana et al. in 1981 [57], suggest that the information for the formation of native structure in integral membrane proteins is contained in their amino acid sequence, as previously described by the Anfinsen paradigm for soluble proteins [58].

6.3.2
Oriented Insertion and Folding into Phospholipid Bilayers

Surrey and Jähnig [51] showed that OmpA spontaneously inserts and folds into phospholipid bilayers. Oriented insertion and folding of OmpA into lipid bilayers in absence of detergent was observed when unfolded OmpA in 8 M urea was reacted with SUVs of dimyristoylphosphatidylcholine (diC$_{14:0}$PC) under concurrent strong dilution of the urea. The insertion of OmpA into vesicles was oriented, because trypsin digestion resulted in a 24-kDa fragment, while the full-length OmpA (35 kDa) was no longer observed. Translocation of the periplasmic domain of OmpA across the lipid bilayer into the inside of the vesicle would have lead to a full protection of OmpA from trypsin digestion. The 24-kDa fragment corresponded to the membrane inserted β-barrel domain (19 kDa) and a smaller part of the periplasmic domain, which was largely digested by trypsin. In contrast, only 50% of detergent-refolded OmpA that was reconstituted into diC$_{14:0}$PC vesicles after refolding into micelles could be digested with trypsin, indicating random orientation of the periplasmic domain inside and outside of the phospholipid vesicles [51]. Since OmpA assumed a random orientation after micelle-bilayer fusion [51], it is unlikely that OmpA would first fold into LPS micelles in the periplasm, which then fuse with the outer membrane as first proposed for PhoE based on the appearance of a folded monomer in mixed micelles of LPS and Triton X-100 *in vitro* [59]. However, a PhoE mutant was later shown to fold *in vivo* and also *in vitro* into LDAO micelles, but not into mixed micelles of Triton X-100 and LPS, leading to doubts about the existence of a folded monomeric intermediate of PhoE in LPS *in vivo* [60].

For direct oriented insertion of OmpA into the bilayers, the preformed lipid-vesicles had to be in the lamellar-disordered (liquid-crystalline) phase and the vesicles had to be sonicated [52, 61]. By contrast, insertion and folding did not complete when the lipid bilayers were in the lamellar-ordered (gel) phase or when refolding attempts were made with $diC_{14:0}PC$ bilayers of large unilamellar vesicles (LUVs) that were prepared by extrusion through membranes of pore size 100 nm [62]. Similarly, folding and trimerization of OmpF [63] was observed after interaction of urea-unfolded OmpF with preformed lipid bilayers in the absence of detergent. Membrane inserted dimers of OmpF were detected transiently. *In vitro*, the folding yields of OmpF into lipid bilayers are small (below around 30%) even under optimized conditions [63] and when compared to OmpA, which quantitatively folds at pH 10.

6.3.3
Assemblies of Amphiphiles Induce Structure Formation in *b*-Barrel Membrane Proteins

To determine basic principles for the folding of β-barrel transmembrane proteins, folding of OmpA was examined with a large set of different phospholipids and detergents at different concentrations [50]. Folding of OmpA was successful with 64 different detergents, and phospholipids that had very different compositions of the polar headgroup did not carry a net charge and had a hydrophobic carbon chain length ranging from seven to 14 carbon atoms. Kleinschmidt et al. [50] demonstrated that for OmpA folding, the concentrations of these detergents or phospholipids must be above the critical micelle concentration (CMC), demonstrating that a supramolecular assembly (micelles or lipid bilayers) with a hydrophobic interior is the minimal requirement for the formation of a β-barrel transmembrane domain. OmpA did not fold into micelles of SDS that have a strong negative surface charge. Kleinschmidt et al. [50] monitored folding of OmpA by circular dichroism (CD) spectroscopy and by electrophoretic mobility measurements. Both methods indicate that after exposure to amphiphiles with short hydrophobic chains (with 14 or fewer carbons), OmpA assumes either both secondary and tertiary structure (i.e. the native state) or no structure at all, dependent on the presence of supramolecular assemblies (micelles, bilayers). Thermodynamically, OmpA folding into micelles is a controlled two-state process [50]. The necessary presence of amphiphiles (lipids, detergents) above the critical concentration for assembly (CCA) to induce the formation of native secondary and tertiary structure in OmpA also indicated that β-barrel structure does not develop while detergent or lipid monomers are adsorbed to a newly formed hydrophobic surface of the protein. [The term CCA is defined here to describe the amphiphile concentration at which a geometrically unique, water-soluble supramolecular assembly is formed, which can be a micelle, a lipid vesicle or even an inverted or cubic lipid phase. The CCA is identical to the CMC in the special case of micelle forming detergents. The CCA does not refer to the formation of random aggregates, e.g. misfolded membrane proteins.] To the

contrary, a hydrophobic core of a micelle or bilayer must be present to allow folding of OmpA. Conlan and Bayley [64] reported later that another OMP, OmpG, folds into a range of detergents such as Genapol X-080, Triton X-100, *n*-dodecyl-*β*-ᴅ-maltoside, Tween 20 and octylglucoside. However, OmpG did neither fold into *n*-dodecylphosphocholine nor into the negatively charged detergents SDS and sodium cholate. Similar to OmpA, the detergent concentrations had to be above the CMC for OmpG folding [64]. Different detergents have also been used for refolding of other *β*-barrel membrane proteins for subsequent membrane protein crystallization (for an overview, see, e.g. [65]).

6.3.4
Electrophoresis as a Tool to Monitor Insertion and Folding of *β*-Barrel Membrane Proteins

SDS-polyacrylamide gel electrophoresis (PAGE) according to Laemmli [66] has been very useful to monitor the folding of OmpA into detergent micelles or lipid bilayers, provided that the samples are not boiled prior to electrophoresis [50–52, 55, 56, 62, 67–69]. If samples are not heat denatured, the folded and denatured OMPs migrate differently. For OmpA, Henning et al. described this property as heat modifiability [55]. It has been reported later also for other OMPs of bacteria such as FhuA [70] or OmpG [26, 64, 71]. Native OmpA, for example, migrates at 30 kDa, whereas unfolded OmpA migrates at 35 kDa [55]. Up to the present, all structural and functional experiments have shown a strict correlation between the 30-kDa form and structurally intact, fully functional OmpA. These previous studies included analysis of the OmpA structure by Raman, Fourier transform IR (FTIR) and CD spectroscopy [50–52, 56, 61, 72], biochemical digestion experiments [51, 67], and functional assays such as phage inactivation [55] and single-channel conductivity measurements [73].

It is possible to determine the kinetics of native structure formation in OmpA (and probably also in other OMPs) using the different electrophoretic mobilities of folded and unfolded OmpA, because OmpA folding can be inhibited by SDS and SDS does not unfold OmpA unless samples are boiled [52, 62, 67]. In an assay to determine the folding kinetics of OmpA, SDS was added to small volumes of the reaction mixture that were taken out at defined times after initiation of folding. In these samples, SDS bound quickly to folded and unfolded OmpA and stopped further OmpA folding [62, 67]. Finally, the fractions of folded OmpA in all samples were determined by cold SDS-PAGE (i.e. without heat-denaturing the samples). The fractions of folded OmpA at each time were estimated by densitometric analyses of the bands of folded and of unfolded OmpA, thus monitoring the formation of tertiary structure in OmpA as a function of time [kinetics of tertiary structure formation by electrophoresis (KTSE)].

6.3.5

pH and Lipid Headgroup Dependence of the Folding of β-Barrel Membrane Proteins

Although OmpA folded quantitatively into a wide range of neutral detergents, it did not fold into negatively charged SDS micelles at neutral or basic pH (cf. [56]). The negative charge of SDS could not be the only reason for lack of folding into these micelles, since OmpA folded partially into micelles of negatively charged LPS at pH 7 [68] and also into bilayers containing negatively charged phosphatidylglycerol [68, 74]. Surrey and Jähnig reported that OmpA folding yields reached 100% in neutral bilayers of $diC_{14:0}PC$ at pH 10, but were only around 70% at neutral pH [52]. The increased folding yield at pH 10 was very likely a consequence of an increased negative surface charge of OmpA (pI=5.9) at pH 10 that increased the solubility of OmpA, i.e. suppresses the aggregation side-reaction. Surrey and Jähnig reported further that OmpA folding yields were again much lower at the even higher pH 12 [52]. They concluded that upon deprotonation of the arginine side-chains of OmpA, the increased negative net charge or negative surface potential of OmpA is too high to allow structure formation. Charge–charge repulsions between the negative surface potential of SDS micelles and negative charges on OmpA might have been the reason why OmpA did not fold into SDS micelles. The relatively small headgroup of SDS in comparison with the negatively charged LPS or phosphatidylglycerol causes a higher charge density on the surface of the SDS micelle, preventing insertion and folding of OmpA, which is negatively charged above pH 5.9.

6.4

Kinetics of Membrane Protein Folding

6.4.1

Rate Law for β-Barrel Membrane Protein Folding and Lipid Acyl Chain Length Dependence

The rate law of OmpA folding into a range of different phospholipid bilayers was determined using the method of initial rates. Kleinschmidt and Tamm [62] found that the folding kinetics of OmpA into LUVs of short-chain phospholipids and also into SUVs of $diC_{18:1}PC$ at 40 °C follow a single-step second-order rate law. The folding kinetics of OmpA could be approximated with a pseudo-first-order rate law, if the lipid concentration was high compared to the protein concentration (above 90 mol lipid mol protein^{-1}). With this approximation, a rate constant was observed that was identical to the product of the second-order rate constant and the lipid concentration. When fitted with a second-order rate law, the kinetic rate constants did neither depend on the lipid nor on the protein concentration, if the lipid/protein ratio was above around 90 mol mol^{-1}, while the first-order rate constant depended on the lipid concentration. However, the second-order rate constants strongly depended on the acyl chain

lengths of the lipids. When OmpA folding into bilayers of $diC_{12}PC$ was monitored by fluorescence spectroscopy, this rate constant was $k_{2ord} \sim 0.4 \, l \, mol^{-1} \, s^{-1}$, while it was $k_{2ord} \sim 5.2 \, l \, mol^{-1} \, s^{-1}$ for OmpA folding into bilayers of $diC_{11:0}PC$ and $k_{2ord} \sim 30 \, l \, mol^{-1} \, s^{-1}$ for OmpA folding into $diC_{10:0}PC$ bilayers [62].

6.4.2
Synchronized Kinetics of Secondary and Tertiary Structure Formation of the *β*-Barrel OmpA

The kinetics of membrane insertion and structure formation of OmpA initiated by denaturant dilution in the presence of preformed lipid bilayers may also be monitored by CD spectroscopy or by KTSE. When the kinetics of secondary structure formation were measured for OmpA insertion and folding into LUVs of saturated short-chain phospholipids, a similar dependence of the rate constants on the length of the hydrophobic acyl chains of the lipids was observed as by fluorescence spectroscopy. However, the second-order rate constants were generally smaller than the corresponding rate constants of the fluorescence time courses [62]. Secondary structure formation was fastest with $diC_{10:0}PC$ and slowest with $diC_{12:0}PC$ as determined from the CD kinetics at 204 nm. When OmpA was reacted with preformed lipid bilayers (LUVs) of $diC_{14:0}PC$ or $diC_{18:1}PC$, the CD signals did not change with time, indicating no changes in the secondary structure of OmpA upon incubation with these lipids.

6.4.3
Interaction of OmpA with the Lipid Bilayer is Faster than the Formation of Folded OmpA

When folding kinetics were analyzed using KTSE assays to determine the rate constants of tertiary structure formation, observations corresponded to those made by CD spectroscopy. The folding kinetics of OmpA were dependent on the length of the hydrophobic chains, but OmpA did not fold when the experiments were performed with $diC_{14:0}PC$ or $diC_{18:1}PC$. The OmpA folding kinetics into $diC_{12:0}PC$ bilayers at different concentrations were fitted to a second-order rate law and second-order rate constants were determined. Over a range of different lipid concentrations, the second-order rate constants obtained by KTSE were practically indistinguishable from the second-order rate constants of secondary structure formation. The rate constants of the secondary and tertiary structure formation of OmpA in $diC_{12:0}PC$ were both $^{s/t}k_{2ord} \sim 0.090 \, l \, mol^{-1} \, s^{-1}$. By contrast, the second-order rate constant obtained from the fluorescence time courses of the OmpA folding kinetics into this lipid was about 4- to 5-fold higher ($^{pla}k_{2ord} \sim 0.4 \, l \, mol^{-1} \, s^{-1}$), indicating that the adsorption and insertion of the fluorescent Trp residues of OmpA into the hydrophobic core of the lipid bilayer were faster than the formation of the fully folded form of OmpA. Four of the five Trps of OmpA are at the front end of the *β*-barrel and presumably interacted first with the hydrophobic core of the membrane, leading to fast fluores-

cence kinetics compared to the CD kinetics and kinetics of tertiary structure formation by electrophoresis. Together, these results indicated that the formation of the β-strands and the formation of the β-barrel of OmpA take place in parallel and are a consequence of the insertion of the membrane protein into the lipid bilayer. The previous observation that a preformed supramolecular amphiphile assembly is necessary for structure formation in OmpA was therefore further detailed by a kinetic characterization of the faster rates of interaction of OmpA with the lipid bilayer and by the slower rates of secondary and tertiary structure formation in OmpA.

6.5
Folding Mechanism of the *b*-Barrel of OmpA into DOPC Bilayers

6.5.1
Multistep Folding Kinetics and Temperature Dependence of OmpA Folding

Early folding experiments with urea-unfolded OmpA and membranes of $diC_{14}PC$ indicated that OmpA folds into lipid bilayers of SUVs prepared by sonication, but not into bilayers of LUVs with a diameter of 100 nm prepared by extrusion [51, 52]. Lipids with longer chains such as $diC_{14:0}PC$ and dioleoylphosphatidylcholine ($diC_{18:1}PC$) required the preparation of SUVs by ultrasonication and temperatures greater than around 25–28 °C for successful OmpA insertion and folding [51, 67].

Lipid bilayers of SUVs have a high surface curvature and intrinsic curvature stress. This leads to an increase of the hydrophobic surface that is exposed to OmpA after it is adsorbed at the membrane water interface, facilitating insertion of OmpA into SUVs compared to insertion of OmpA into bilayers of LUVs, where curvature stress is much lower and no insertion was observed. The folding kinetics of OmpA into SUVs of $diC_{14:0}PC$ or $diC_{18:1}PC$ were slower compared to the folding kinetics into LUVs short chain phospholipids and strongly temperature dependent [62]. The fluorescence kinetics of OmpA folding that could still be fitted to a single-step pseudo first-order rate law at 40 °C [62, 67] were more complex when the temperature for folding was 30 °C or less. A single-step rate law was not sufficient to describe the kinetics [67]. Insertion and folding of OmpA into bilayers of $diC_{18:1}PC$ (SUVs) was characterized by at least three kinetic phases, when experiments were performed at temperatures between 2 and 40 °C. These phases could be approximated by pseudo-first-order kinetics at a lipid/protein ratio of 400. Two folding steps could be distinguished by monitoring the fluorescence time courses at 30 °C. The first (faster) step was only weakly temperature dependent ($k_1 = 0.16$ min^{-1} at 0.5 mM lipid). The second step was up to two orders of magnitude slower at low temperatures, but the rate constant approached the rate constant of the first step at higher temperatures (around 0.0058 min^{-1} at 2 °C and around 0.048–0.14 min^{-1} at 40 °C, in the presence of 0.5 mM lipid). The activation energy for the slower process was

46 ± 4 kJ mol^{-1} [67]. An even slower phase of OmpA folding was observed by KTSE assays, indicating that tertiary structure formation was slowest with a rate constant $k_3 = 0.9 \times 10^{-2}$ min^{-1} (at 3.6 mM lipid and at 40 °C) [67]. This is consistent with the smaller rate constants of secondary and tertiary structure formation in comparison to the rate constants of protein association with the lipid bilayer, which were later observed for OmpA folding into LUVs of short-chain phospholipids [62] (see Section 6.4.3). The kinetic phases that were observed for OmpA folding into diC$_{18:1}$PC bilayers (SUVs) suggest that at least two membrane-bound OmpA folding intermediates exist when OmpA folds and inserts into lipid bilayers with 14 or more carbons in the hydrophobic acyl chains. These membrane-bound intermediates could be stabilized in fluid diC$_{18:1}$PC bilayers at low temperatures between 2 and 25 °C (the temperature for the phase transition of diC$_{18:1}$PC from the lamellar-ordered to the lamellar-disordered liquid-crystalline phase is $T_c = -18$ °C). The low-temperature intermediates could be rapidly converted to fully inserted, native OmpA, as demonstrated by temperature jump experiments [67].

6.5.2
Characterization of Folding Intermediates by Fluorescence Quenching

Tryptophan fluorescence quenching by brominated phospholipids (see, e.g. [75–82]) or by lipid spin-labels (see, e.g. [83–88]) traditionally has been very valuable to determine characteristic elements of the transmembrane topology and lipid–protein interactions of integral membrane proteins. To further characterize the folding process of OmpA, we combined this method with the study of the folding kinetics of OmpA into bilayers (SUVs) of diC$_{18:1}$PC [89, 90]. The average positions of the five fluorescent Trps of OmpA were characterized for the membrane-bound folding intermediates that were previously implicated by the discovery of multistep folding kinetics [67]. A new method was developed by studying the kinetics of the refolding process in combination with the Trp fluorescence quenching at different depths in the lipid bilayer [90] using membrane embedded quenchers. The positions of fluorescent Trps with reference to the center of the phospholipid bilayer can be determined using a set of membrane integrated fluorescence quenchers that carry either two vicinal bromines or alternatively a doxyl group at the *sn*-2 acyl chain of the phospholipid. When in close proximity to the fluorescent Trp residues of integral membrane proteins, these groups quench the Trp fluorescence. The positions of the bromines in 1-palmitoyl-2-(4,5-dibromo-)stearoyl-*sn*-glycero-3-phosphocholine (4,5-DiBrPC), 6,7-DiBrPC, 9,10-DiBrPC and 11,12-DiBrPC are known from X-ray diffraction to be 12.8, 11.0, 8.3 and 6.5 Å from the center of the lipid bilayer [91, 92]. The fluorescence intensity of the Trps of OmpA was measured as a function of time after initiation of OmpA folding by dilution of the denaturant in presence of preformed lipid bilayers containing one of the brominated lipids as a fluorescence quencher. In a set of four equivalent folding experiments, bilayers were used that contained 30 mol% of one of the four brominated lipids and 70%

diC$_{18:1}$PC. The fluorescence intensities in the four different time courses of OmpA folding in presence of each of the four brominated lipids were subsequently normalized by division with fluorescence intensities obtained upon OmpA folding into bilayers of 100% diC$_{18:1}$PC (i.e. in the absence of any quencher). Thus, depth-dependent quenching profiles were obtained at each time after initiation of OmpA folding. From these profiles, the vertical location of Trp in the membrane in projection to the bilayer normal was then determined using the parallax method [88, 93] or the distribution analysis [81, 82].

A large set of experiments was performed in the temperature range between 2 and 40 °C. At each selected temperature, the average distances of the Trps to the center of the lipid bilayer were determined as a function of time. Therefore, we called this method time-resolved distance determinations by Trp fluorescence quenching (TDFQ) [90]. Previously unidentified folding intermediates on the pathway of OmpA insertion and folding into lipid bilayers were detected, trapped and characterized. Three membrane-bound intermediates were described, in which the average distances of the Trps from the bilayer center were 14–16, 10–11 and 0–5 Å, respectively [90]. The first folding intermediate was stable at 2 °C for at least 1 h. A second intermediate was characterized at temperatures between 7 and 20 °C. The Trps moved 4–5 Å closer to the center of the bilayer at this stage. Subsequently, in an intermediate that was observed at 26–28 °C, the Trps moved another 5–11 Å closer to the center of the bilayer. This intermediate appeared to be less stable. The distribution parameter, calculated from distribution analysis, was largest for the Trp distribution of this intermediate. This was a consequence of the mechanism of folding and of the structure of folded OmpA [3, 4, 94]. The large distribution parameter observed for this intermediate was consistent with experiments on single Trp mutants of OmpA [89] (see below). Trp7 has to remain in the first leaflet of the lipid bilayer, while the other Trps must be translocated across the bilayer to the second leaflet. Therefore, with symmetrically incorporated brominated lipids as fluorescence quenchers, the largest distribution parameter was observed when the four translocating Trps are in the center of the lipid bilayer. Formation of the native structure of OmpA was observed at temperatures above about 28 °C. In the end of these kinetic experiments, all five Trps were finally located on average about 9 to 10 Å from the bilayer center, Trp7 in the periplasmic leaflet and the other four Trps in the outer leaflet of the outer membrane.

When KTSE experiments were performed to monitor OmpA folding at 30 °C, a 32-kDa band was observed in the first few minutes of OmpA folding [67]. The folding conditions for this experiment were nearly identical to those of the fluorescence quenching experiments at 28–30 °C. Therefore, this 32-kDa form is very likely identical to the third folding intermediate of OmpA, in which the average Trp-location is 0–5 Å from the center of the lipid bilayer. The comparison indicated that in this intermediate, a significant part of the β-barrel had formed, which is resistant to treatment with SDS at room temperature.

6.5.3
The β-Barrel Domain of OmpA Folds and Inserts by a Concerted Mechanism

TDFQ experiments were subsequently performed with the five different single Trp mutants of OmpA. These mutants were prepared by site-directed mutagenesis [89], and contained each a single Trp and four phenylalanines in the five Trp positions of the wild-type protein. All mutants were isolated from the *E. coli* outer membrane and refolded *in vitro* into lipid bilayers. Time-resolved distance determinations (TDFQ) for each of the single Trp mutants of OmpA gave more structural detail on the folding mechanism of OmpA. TDFQ experiments were carried out at selected temperatures between 2 and 40 °C [89]. When kinetic experiments were performed below 30 °C, each of the five Trps approached a distance of 10–11 Å from the bilayer center in the end of the fluorescence time course of OmpA folding. The distance decrease with time was observed even at 40 °C for Trp7. The TDFQ results showed that Trp7 did not migrate any closer to the bilayer center than around 10 Å independent of the experimental conditions. However, Trp15, Trp57, Trp102 and Trp143 were detected very close to the center of the lipid bilayer in the first minutes of refolding at temperatures of 30, 32, 35 and 30 °C, respectively. TDFQ experiments performed at 40 °C resolved the last two steps of OmpA refolding, and the translocation rate constants of the first phase of fast distance change were 0.55, 0.46, 0.26 and 0.43 min^{-1} for Trp15, Trp57, Trp102 and Trp143, respectively. The four Trps crossed the center of the bilayer and approached distances of around 10 Å from the bilayer center in the final folding step of OmpA. These experiments demonstrated that Trp15, Trp57, Trp102 and Trp143 are similarly located in three folding intermediates that were also observed previously for wild-type OmpA. The similar distances of these Trps from the membrane center in each of the membrane-bound folding intermediates indicate a simultaneous translocation of the transmembrane segments of OmpA, coupled to the formation of the β-barrel structure upon insertion.

The results of these kinetic studies on the folding mechanism of OmpA may be used to develop a tentative model of OmpA folding (Fig. 6.2): the time courses of OmpA folding into phospholipid bilayers (LUVs) of $diC_{12:0}PC$ indicated that β-strand secondary and β-barrel tertiary structure formation are synchronized with the same rate constant [62], which is lower than the rate constant of the fluorescence time course of OmpA adsorption to the lipid bilayer. Strongly temperature dependent kinetics were observed and several kinetic phases were distinguished, when folding of OmpA was investigated with lipid bilayers of $diC_{18:1}PC$ (SUVs), which is a phospholipid with comparably long hydrophobic chains. OmpA first adsorbs to the water–membrane interface (intermediate A) and the intrinsic fluorescence of OmpA increases strongly due to the partitioning of the fluorescent Trps into the less polar environment at the membrane–water interface. Subsequently, the slower phase of the fluorescence changes reflect the migration of the Trps from the membrane–water interface into the hydrophobic core of the lipid bilayer. The translocation of the Trps across the bilayer is best monitored with membrane inserted fluorescence
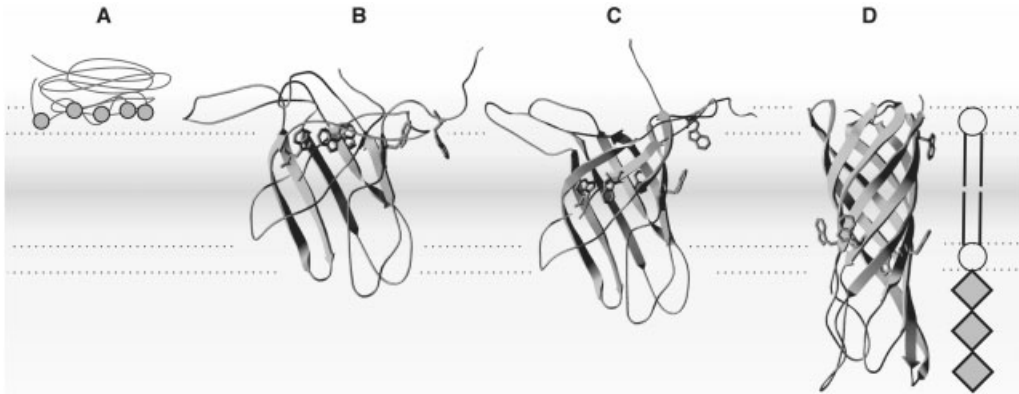
Locations of the Tryptophans of OmpA in Folding Intermediates identified by TDFQ:

Distance to the Center of the Lipid Bilayer

Tryptophan	I_{M1} (A) $\longrightarrow$	I_{M2} (B) $\longrightarrow$	I_{M3} (C) $\longrightarrow$	N (D)
7	~14-16 Å	~10 Å	~10 Å	~10 Å
15, 57, 102, 143		~10 Å	~0-5 Å	~10 Å

Fig. 6.2 Folding model of OmpA. The kinetics of β-sheet secondary and β-barrel tertiary structure formation in OmpA have the same rate constants and are coupled to the insertion of OmpA into the lipid bilayer [62, 89, 90]. The locations of the five Trps in the three identified membrane-bound folding intermediates and in the completely refolded state of OmpA [89, 90] are shown. Additional details, such as the translocation of the long polar loops across the lipid bilayer, must still be determined. OmpA structures were generated with DeepView [146, 147].

quenchers, since the intrinsic Trp fluorescence does not change much during Trp migration through the 30-Å hydrophobic core of $diC_{18:1}$PC. The average location of the Trps of 14–16 Å from the bilayer center after adsorption to the membrane-water interface was determined by TDFQ experiments at 2 °C [90]. At temperatures of 5–25 °C, this initial phase of folding was fast and followed by a second, slower phase, in which the Trps move into more hydrophobic regions at a distance of about 10 Å from the bilayer center. The observed folding intermediate (B) is quite stable. A third membrane-bound intermediate (C) was identified at 27–29 °C. In this intermediate, all Trps, except Trp7, are detected a distance of 0–5 Å from the bilayers center in the first minutes of OmpA folding. Trp7 remains at the same location as in intermediate B. Very likely, this intermediate is identical to the 32-kDa form of OmpA that was previously observed by KTSE experiments [67]. Finally, at temperatures above 28–30 °C, Trp15, Trp57, Trp102 and Trp143 move away from the center of the bilayer to a distance of about 10 Å. This distance of the Trp residues of OmpA compares well with the X-ray and nuclear magnetic resonance structures of OmpA [3, 4]. The basic elements of the model in Fig. 6.2 are the synchronized kinetics of second-

ary and tertiary structure formation, the simultaneous migration of the Trps that cross the bilayer center, and the migration of Trp7, which does not translocate. However, more structural information is needed to improve this preliminary model. For example, it is not known how the residues of the polar loops of OmpA cross the hydrophobic core of the lipid bilayer.

6.6
Protein–Lipid Interactions at the Interface of *β*-Barrel Membrane Proteins

6.6.1
Stoichiometry of the Lipid–Protein Interface

To resolve the interactions between membrane lipids and fully inserted and folded *β*-barrel membrane proteins in detail, Ramakrishnan et al. [95] investigated the stoichiometry and lipid selectivity of the eight-stranded OmpA and the 22-stranded FhuA in dimyristoylphosphatidylglycerol ($diC_{14:0}$PG) bilayers by electron spin resonance (ESR) spectroscopy, a method that was very successfully applied previously to investigate lipid–protein interactions of *α*-helical membrane proteins (see, e.g. [96]). Spin-labeled lipids of different headgroup compositions, but with the same fatty acyl chains, were incorporated into $diC_{14:0}$PG bilayers with either OmpA or FhuA. ESR spectra of bilayers containing 1 mol% of phosphatidylglycerol carrying the doxyl group at C-14 of the *sn*-2 acyl chain (14-PGSL), were recorded at 30 °C, i.e. above the gel-to-liquid-crystalline phase transition temperature of $diC_{14:0}$PG. Difference spectroscopy demonstrated that the spectra had two components when either OmpA or FhuA was present in the lipid bilayer. The two components corresponded to protein-immobilized lipid spin-labels and to mobile spin-labels in the $diC_{14:0}$PG host matrix. Similar components of spin-label spectra were described previously in a wide range of studies with *α*-helical membrane proteins [96–99]. The ratio of mobile/immobile lipid populations was proportional to the lipid/protein ratio. From this linear dependence, it was possible to calculate the number of lipids in contact with the protein. Stoichiometries of 11 lipids/OmpA and of 32 lipids/FhuA, respectively, were found for the protein–lipid molecular interface [95].

6.6.2
Lipid Selectivity of *b*-barrel Membrane Proteins

The ESR spectra also demonstrated that lipids with different chemical structure of their polar headgroups have different affinities to associate with the integral *β*-barrel membrane proteins. A quantitative analysis of the ESR spectra resulted in the relative association constants of the different lipid species with FhuA and OmpA [95]. For OmpA, the lipid headgroup selectivity was phosphatidic acid → phosphatidylglycerol → phosphatidylcholine → phosphatidylethanolamine → phosphatidylserine → di acylglycerol → stearic acid. For FhuA, the selectivity pattern was stearic acid → phosphatidic acid → phosphatidylcholine → phospha-

tidylglycerol → phosphatidylserine → phosphatidylethanolamine → diacyl glycer-ol. The strong difference in the selectivity for stearic acid was explained by a different protonation state of stearic acid in association with OmpA as compared to FhuA in the negatively charged $diC_{14:0}PG$ host bilayer. Since $diC_{14:0}PG$ bilayers have a strongly negative electrostatic surface potential, stearic acid is expected to be protonated at pH 7. In reconstituted bilayers of FhuA, the negative surface potential is locally neutralized in regions of high positive charge on FhuA, leading to the ionized form of stearic acid [100]. Representations of the surface electrostatics of the crystal structures of OmpA and FhuA indicate an excess of positive charges on the extracellular, but not on the periplasmic surface of the two proteins, which is more pronounced for FhuA. This may explain the overall selectivity of these β-barrels for negatively charged lipids. On the extracellular side of OmpA, basic side-chains, $Lys64(\beta_3)$, $Lys73(\beta_4)$, $Arg103(\beta_5)$ and $Lys113(\beta_6)$ are located in extensions of the β-strands facing the lipid headgroup region. These side-chains may probably cause the observed selectivity of OmpA for the negatively charged phospholipids. It is likely that this cluster of positively charged lysine and arginine residues also forms a binding site for the negatively charged LPS, similar to the one identified in FhuA [24, 101], which contains $Lys306(\beta_7)$, $Lys351(\beta_8)$, $Arg382(\beta_9)$ and $Lys437(\beta_{10})$. FhuA also has a marked selectivity for negatively charged phospholipids [95]. For both OmpA and FhuA, the relative association constant for phosphatidylglycerol is about 2 times greater than the relative association constant of phosphatidylethanolamine, indicating that phosphatidylglycerol is the preferred lipid at the interface to the OMPs in the outer membranes of bacteria, especially in mutant strains that do not contain LPS [102, 103]. Similar clusters of positively charged residues that form a binding site for negatively charged LPS have also been observed in other OMPs such as OmpT [104, 105].

6.7
Orientation of β-Barrel Membrane Proteins in Lipid Bilayers

6.7.1
Lipid Dependence of the β-Barrel Orientation Relative to the Membrane

The orientation of the β-barrel membrane proteins OmpA and FhuA and their order parameters have been determined recently from IR dichroism studies [100]. The tilt angle of the barrel axis relative to the membrane normal, α (i.e. the mean effective inclinations of the β-sheets relative to the membrane normal), depended on the thickness of the lipid bilayer and decreased in fluid bilayers from $\alpha=45°$ for $diC_{12:0}PC$ to $\alpha=30°$ for $diC_{17:0}PC$ in case of the eight-stranded β-barrel domain of OmpA (residues 0–176 of OmpA). The barrel tilt angle, α, was generally smaller for the 22-stranded β-barrel domain of FhuAΔ5–160, ranging from $\alpha=36°$ in $diC_{12:0}PC$ to $\alpha=21°$ in $diC_{17:0}PC$. The protein order parameters in these fluid bilayers increased for OmpA0–176 from 0.25 (in $diC_{12}PC$) to 0.61 (in $diC_{17:0}PC$) and increased for FhuAΔ5–160 from 0.48 (in

diC$_{12}$PC) to 0.80 (in diC$_{17:0}$PC). The lipid order parameters exhibited little systematic change with lipid chain length [100]. Also, in the case of OmpA and OmpA0–176, differences between data for fluid and gel-phase bilayers were not large, but barrel tilts were considerably smaller and order parameters larger for FhuAΔ5–160 in fluid than in gel-phase bilayers. The greater freedom of orientation of OmpA in thin lipid bilayers correlates well with faster rates of insertion and folding observed with thin bilayers [62]. Since the β-barrel domain of FhuA has a much larger cross-section (39 Å×46 Å [24]) than OmpA (with an outer diameter of 24 Å [94]), the membrane ordering is greater for FhuA [100].

6.7.2
Inclination of the β-Strands Relative to the β-Barrel Axis in Lipid Bilayers

The tilt angles, β, of the β-strands relative to the barrel axis were $\beta=44°$ for OmpA0–176 and $\beta=44.5°$ for FhuAΔ5–160, when determined from attenuated total internal reflection (ATR)-FTIR spectra. For comparison, strand tilt angles relative to the barrel axis were $\beta=43.1°$ for OmpA0–171 [4, 94, 106] and $\beta=38.3$ for FhuAΔ5–160 [24, 106] when calculated from the crystal structures. The slightly larger strand tilts obtained for FhuA were interpreted as a slight relaxation of the FhuAΔ5–160 structure relative to the packing of the whole protein in the crystal [100]. Ramakrishnan et al. [100] also estimated the sheet twist, $\theta=18°$ (wt-OmpA) and $\theta=6°$ (FhuAΔ5–160), and strand coiling, $\varepsilon=10°$ (wt-OmpA) and $\varepsilon=4°$ (FhuAΔ5–160) from the β-strand tilts, β, that were obtained from the dichroic ratios of ATR-FTIR spectra. The values were in agreement with the estimates from the X-ray crystal structures, suggesting similar β-barrel geometries of OmpA and FhuA in lipid membranes and X-ray crystals.

Analysis of the FTIR spectra of wt-OmpA and OmpAΔ5–160 [100] showed that the overall percentage of β-sheet secondary structure in wt-OmpA was 59%, while a β-sheet content of 63% was deduced from the crystal structure of OmpA0–171 [4]. Ramakrishnan et al. [100] therefore concluded that about 55% of the periplasmic domain of OmpA must also be of β-sheet secondary structure. Interestingly, the crystal structure of the 127 residue C-terminal domain of RmpM, which is homologous to the periplasmic domain of OmpA with about 35% sequence identity, contains 25% β-strands and 25% β-turns [107].

6.7.3
Hydrophobic Matching of the β-Barrel and the Lipid Bilayer

The tilts of the strands can be used to deduce information about the hydrophobic thickness of lipid bilayer. The hydrophobicity analysis [72] of the OmpA barrel showed that the hydrophobic region, which is delimited by two aromatic girdles, is comprised of an average of five outward facing residues in each of the strands of the OmpA transmembrane domain. With the rise of 3.45 Å per residue [108] and an average tilt angle of 44°, the hydrophobic thickness can be estimated to around 25 Å, which agrees well with estimates for several OMPs of

E. coli [109]. When the acyl chain length dependence of the lipid affinity of another OMP, OmpF, was investigated by fluorescence spectroscopy [110], a maximum affinity was found for $diC_{14:1}PC$, with a progressive decrease for lipids with longer acyl chains. The double bond reduces the bilayer thickness, which is comparable for $diC_{14:1}PC$ and $diC_{12:0}PC$ [111], to about 24 nm. This is consistent with the thickness derived from β-strand tilt angles.

6.8
In vivo Requirements for the Folding of OMPs

6.8.1
Amino Acid Sequence Constraints for OmpA Folding *in vivo*

Koebnik [112] tested constraints within the amino acid sequence that limit the folding of OmpA *in vivo*. In this study, OMPs assembled efficiently into the outer membrane only when at least four of the five residues pointing to the hydrophobic chains of the membrane lipids were hydrophobic. In addition, none of the three central residues of a β-strand could be charged. The amino acid side-chains facing the inside of the small eight-stranded β-barrel of OmpA could not be large and proline residues were not well tolerated in the β-strands.

Two complementary OmpA fragments that were split at the second or third periplasmic turn could be co-expressed in *E. coli* and assembled efficiently with all termini located in the periplasmic space [113]. When pairs of the transmembrane β-strands were permuted on the DNA level, only the three possible circular permutations led to correctly assembled OmpA variants, although their assembly was less efficient than the assembly of OmpA [114].

6.8.2
Periplasmic Chaperones

The biochemical requirement for the *in vitro* folding of β-barrel membrane proteins OmpA [50, 56], OmpG [64], OmpF [63], PhoE [115] and others from a denatured state in urea appears to be a supramolecular assembly of amphiphiles [50, 69]. While the presence of a supramolecular assembly of detergents or lipids is a minimal requirement for the *in vitro* folding of β-barrel membrane proteins such as OmpA, additional components may be necessary *in vivo*. For instance, it is not clear how OMPs are successfully targeted to the outer membrane, and how insertion and finally folding of other OMPs takes place, which exhibited poor folding yields *in vitro*, such as OmpF [63] and FhuA (Pocanschi and Kleinschmidt, in preparation). Poor *in vitro* refolding upon denaturant dilution in presence of preformed phospholipid bilayers appears to be a consequence of the fast aggregation of OMPs, which competes with bilayer insertion and folding. *In vivo*, molecular chaperones keep the OMPs soluble in the periplasm [116, 117] before they become part of the outer membrane. The chaper-

ones are likely more efficient to prevent OMP aggregation in comparison to the denaturant urea that has been used in folding studies *in vitro* and that must be diluted before OMPs can insert and fold into model membranes. *In vivo*, there must also be a targeting mechanism that prevents the insertion of OMPs from the periplasm into the cytoplasmic membrane and specifically directs them to the outer membrane. It may be possible that differences in the physicochemical properties of the inner and outer membrane are responsible for the targeting of β-barrel membrane proteins to the outer membrane. For instance, the average hydrophobic thicknesses of the proteins of the outer membrane (22–24 Å) [62, 109] and of the inner membrane (around 26–29 Å) [109] of *E. coli* are different. In fact, *in vitro* experiments also showed that insertion and folding of OmpA into thin membranes are faster then into phospholipid bilayers with a thicker hydrophobic core [62]. The outer membrane contains mostly LPS in the outer leaflet. LPS has relatively short hydrocarbon chains, which are partially hydroxy-lated close to the glucosamine backbone at C-3, lowering the hydrophobic thickness of the outer membrane. Whether this difference in the hydrophobic thicknesses of the inner and outer membranes is really relevant for targeting of OMPs to the outer membrane, remains to be clarified. Most likely, proteins are involved in proper targeting of OMPs to the outer membrane. Several periplasmic proteins and LPS have been demonstrated to interact with OMPs in the periplasm. OMPs of Gram-negative bacteria are translocated across the cytoplasmic membrane into the periplasm in a mostly unfolded form by the SecA/E/Y/G export system (for recent reviews, see, e.g. [118, 119]). In the periplasm, the signal sequence is cleaved off by a signal peptidase. Genetic studies on possible periplasmic chaperones and biophysical assays with these chaperones and soluble proteins as their substrates suggested that for example SurA (45 kDa) [120–122] and FkpA (26 kDa) [123–125] have a role in the targeting and assembly of OMPs. In these studies, the periplasmic chaperones prevented the aggregation of soluble proteins. *In vivo*, the concentrations of some OMPs in the outer membrane of *E. coli* were decreased, when the genes of the periplasmic proteins Skp [46] or SurA [120, 121] were deleted. Representatives of three different families of peptidyl-prolyl *cis/trans* isomerases were found in the periplasm. Examples are the parvulin-type SurA [122, 123], the FKBP-type FkpA [123–126] and the cyclophilin-type PpiA (RotA, 18 kDa) [127]. SurA bound the 18-stranded LamB *in vitro* [122].

6.8.3
Insertion and Folding of the β-Barrel OmpA is Assisted by Skp and LPS

Direct biochemical evidence for a chaperone-assisted three-step delivery pathway of OmpA to a model membrane was first given by Bulieris et al. [68]. It was demonstrated that the periplasmic chaperone Skp [116, 128–131] keeps OmpA soluble *in vitro* at pH 7 in an unfolded form even when the denaturant urea was diluted out. Skp was also shown to prevent the premature folding of OmpA into LPS micelles and to inhibit the folding of OmpA into phospholipid bilayers composed of phosphatidylethanolamine, phosphatidylglycerol and phosphatidylcholine [68].

Only when Skp complexes with unfolded OmpA were reacted with LPS in a second stage, a folding competent form of OmpA was formed that efficiently inserted and folded into phospholipid bilayers in a third stage. In this Skp/LPS-assisted folding pathway, Bulieris et al. observed faster folding kinetics and higher yields of folded OmpA in comparison to the direct folding of OmpA into the same lipid bilayers upon urea dilution in absence of Skp and LPS. In the sole presence of either Skp or LPS, the kinetics of insertion and folding were inhibited (Fig. 6.3). The higher folding yields of OmpA from the complex with Skp and LPS (in comparison to OmpA folding from the urea denatured state) may be a consequence of faster Skp binding to unfolded OmpA in solution in comparison to the folding of OmpA into lipid bilayers. Faster rates of Skp binding in solution would result in relatively lower amounts of aggregated OmpA, thus increasing the amounts of OmpA available for folding. However, Bulieris et al. [68] also showed that LPS is required for the efficient OmpA insertion from complexes with Skp into lipid bilayers. In their study, unfolded OmpA bound LPS or Skp or both. The binding stoichiometries were 25 molecules of LPS with a binding constant of
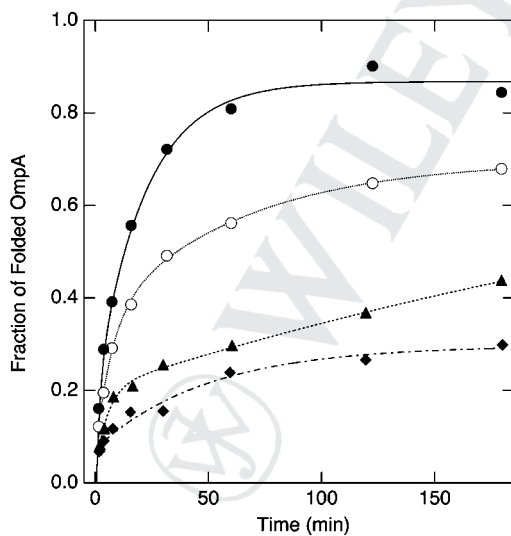

Fig. 6.3 Folding of OmpA into lipid bilayers requires both, Skp and LPS (adapted from [68]). Data shown correspond to Omp folding experiments into lipid bilayers, 30 min after dilution of the denaturant urea, in the absence of Skp and LPS (open circles), in the presence of Skp (diamonds), in the presence of LPS (triangles), and in the presence of both Skp and LPS (solid circles). The folding kinetics were fastest and folding yields were highest when both Skp and LPS were present. Folding was inhibited when either Skp or LPS were absent. The folding kinetics in presence of Skp and LPS also compare favorably with the folding kinetics from the urea-denatured state in the absence of Skp and LPS, indicating that OmpA is insertion competent *in vivo*, in the absence of urea, when in complex with Skp and LPS. The work also indicated that OmpA did not develop native structure when complexed with Skp and LPS, but only in the presence of lipid bilayers.

$K_{\mathrm{LPS}} \sim 1.2 \pm 0.7$ mM^{-1} (i.e. with a free energy of binding $\Delta G = -8.3 \pm 0.3$ kcal mol^{-1}) and three molecules of Skp with a much larger binding constant of $K_{\mathrm{Skp}} \sim 46 \pm 30$ mM^{-1} (i.e. with $\Delta G = -10.3 \pm 0.5$ kcal mol^{-1}) [68]. The 8- to 150-fold greater OmpA binding constant of Skp explains that Skp prevents the folding of OmpA upon addition of LPS micelles. However, LPS was necessary to promote efficient folding of OmpA into preformed phospholipid membranes at optimal stoichiometries of 0.5–1.7 mol LPS mol Skp^{-1} and 3 mol Skp mol unfolded OmpA^{-1}. For fast kinetics and high yields of membrane insertion and folding of OmpA, about 1.5–5 mol LPS bound to Skp/OmpA complexes (i.e. much lower amounts than observed in absence of Skp) [68]. Interestingly CD spectroscopy and KTSE assays indicated that large amounts of secondary and tertiary structure in OmpA only form in the third stage of the assembly pathway, upon addition of phospholipid bilayers [68], suggesting that Skp and LPS deliver OmpA to the membrane, which is absolutely needed for the formation of secondary and tertiary structure in OmpA.

The interaction of the OmpA/Skp/LPS complex with the lipid bilayer is apparently the most important event to initiate folding of OmpA in presence of chaperones and LPS as a folding catalyst. The described assisted folding pathway and discovered 3:1 stoichiometry for Skp binding to OmpA [68] was later supported by the observation that Skp is trimeric in solution [132] and by the description of the crystal structure of Skp and a putative LPS binding site in Skp [133, 134] (Fig. 6.4 A). One LPS binding site per Skp monomer is consistent with the observation of optimal folding kinetics of OmpA from an OmpA/Skp/LPS complex at 0.5–1.7 mol LPS mol Skp^{-1} [68]. In this case, a 1:1 stoichiometry perhaps indicates that LPS only binds to the LPS binding site of Skp and OmpA is completely shielded from interactions with LPS. A current folding model for this assisted OmpA folding pathway is shown in Fig. 6.5.

A second periplasmic protein, the survival factor A, SurA [123], has been demonstrated to affect OMP assembly. *E. coli* mutants, in which the *surA* gene was deleted, had reduced concentrations of OmpA and LamB in the outer membrane [120, 121]. SurA functions as a peptidyl-prolyl *cis/trans* isomerase and as a molecular chaperone [122]. The crystal structure of SurA [135] is shown in Fig. 6.4 B. Genetic evidence suggests that SurA and Skp act as chaperones that are involved in parallel pathways of OMP targeting to the outer membrane [136].

6.8.4
Role of Omp85 in Targeting or Assembly of β-Barrel Membrane Proteins

The Skp/LPS-assisted folding pathway is not the only pathway for OMP folding, because in initial experiments, the folding of the 22-stranded β-barrel FhuA was not facilitated in the presence of Skp and LPS (Pocanschi and Kleinschmidt, unpublished data). There is genetic evidence for a parallel folding pathway involving the periplasmic SurA. The double deletion of the genes *skp* and *surA* is lethal to the bacteria [122, 136]. Also, the assembly of TolC does neither require
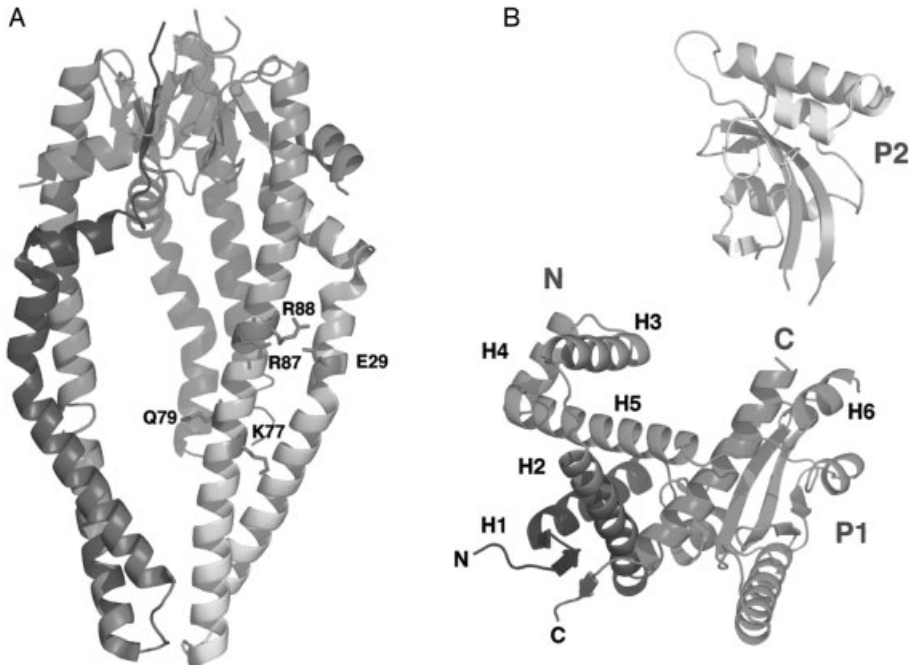
Fig. 6.4 (A) Crystal structure of the Skp trimer (PDB entry 1SG2 [134]). The Skp trimer consists of a tightly packed 12-stranded β-barrel that is surrounded by C-terminal α-helices of the three subunits that point away from the barrel in form of tentacles that are about 65 Å long. These tentacles form a cavity that may take up the unfolded OMP. The outside surface of the helical domain of Skp is highly basic. Each monomer of the trimeric Skp has a putative LPS binding site [133] (Skp structure entry 1UM2 in the PDB). The LPS-binding site was found using a previously identified LPS-binding motif [101], and consists of K77, R87 and R88. This motif matches the LPS-binding motif in FhuA with residues K306, K351 and R382 (see Section 6.6.2) and a root mean square deviation of 1.75 Å for the Cα–Cγ atoms was calculated [133]. Q99 in Skp may also form a hydrogen bond to an LPS phosphate, completing the four-residue LPS-binding motif. (B) Crystal structure of survival factor A, SurA (PDB entry 1M5Y [135]). The N-terminal domain (N) is composed of the α-helices H1 to H6 (residues 1–148) and connected to peptidyl-prolyl *cis/trans* isomerase (PPI) domain P1 (residues 149–260). The P2 domain (residues 261–369) connects to the C-terminal domain C (residues 370–428, colored in red). It has been demonstrated that a mutant SurAN(-Ct), which does not contain the two PPIase domains and is composed of the N and C domains only, functions like a chaperone [122]. This SurA "core domain" has been proposed to bind the tripeptide motif aromatic–random–aromatic, which is prevalent in the aromatic girdles of β-barrel membrane proteins [148]. Figures were created with PyMOL [149].
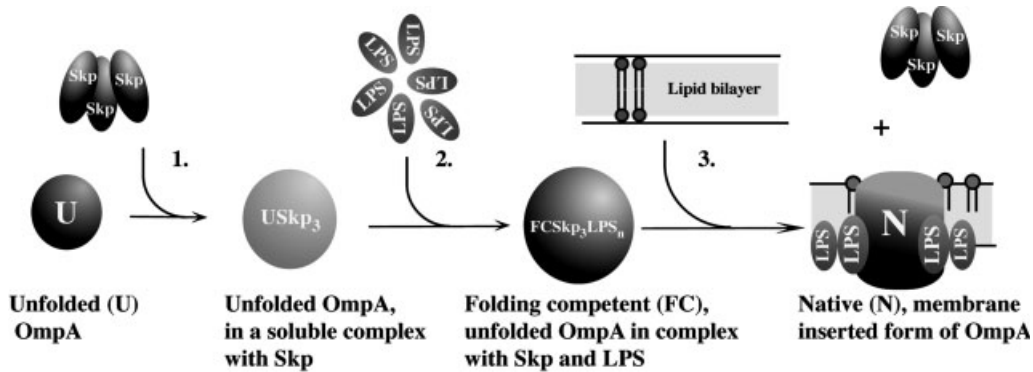
Fig. 6.5 A model of the Skp/LPS-assisted folding pathway of the β-barrel protein OmpA of the outer membrane of *E. coli* is depicted. After translocation across the cytoplasmic membrane by the SecA/E/G/Y system in unfolded form (U), OmpA binds three molecules of the trimeric Skp, which is a periplasmic chaperone and keeps OmpA soluble in an unfolded state (USkp$_3$). The complex of unfolded OmpA and Skp interacts with LPS molecules to form a folding competent intermediate of OmpA (FCSkp$_3$LPS$_n$). In the final step, folding competent OmpA inserts and folds into the lipid bilayer (adapted from [69]).

Skp nor SurA [137]. Recently, an OMP, Omp85, has been demonstrated to be essential for the targeting of integral membrane proteins to the outer membrane [138] and, similarly, Tob55 has been demonstrated to be essential for targeting porins to the outer membrane of mitochondria [139, 140]. Omp85 was necessary for the viability of the bacteria and deletion of the *omp85* gene from the chromosome lead to an accumulation of OMPs in non-native, probably aggregated form. The lack of insertion of the OMPs was further confirmed by immunofluorescence microscopy, which showed strongly reduced surface labeling with antibodies directed against OMPs. Omp85 may therefore be involved either in targeting of OMPs towards or in OMP insertion into the outer membrane, or in both. Alternatively, it was also suggested that the effect of Omp85 may be an indirect one and that Omp85 is instead involved in lipid transport to the outer membrane [141]. This role for Omp85 was proposed, because the *omp85* gene is co-transcribed with several downstream genes involved in lipid or LPS synthesis. Also, OMPs still appeared in fractions of the high density outer membrane fraction after sucrose density centrifugation, while LPS and phospholipids accumulated in the lower density inner membrane fraction, arguing against a role of Omp85 in OMP assembly according to ref. [141]. However, the gene cluster that includes *omp85* also includes *skp*, which codes for the chaperone Skp that is well known for its role in OMP transport [68, 116, 130], but also has a binding site for LPS [133]. Based on the elimination of OMPs from the outer membrane after deletion of the gene for Omp85, it has been proposed that prior to folding, OMPs first insert into a channel formed by the membrane-embedded domain of Omp85, which then laterally opens to allow the stable insertion of

the OMP into the bilayer of the membrane [142]. The proposed role of Omp85 as a translocon-like channel for OMP assembly raises several interesting questions: As has been recently pointed out [143], the lateral opening of the transmembrane channel would involve breaking several hydrogen bonds between the transmembrane β-strands of Omp85, a process that is energetically very unfavorable in the hydrophobic lipid environment of the membrane. If individual β-strands would be released from the Omp85 transmembrane channel, the hydrophilic residues and the polar amide and carbonyl groups of these strands would be exposed to the hydrophobic membrane environment in addition to those of the laterally opened Omp85 channel. On the other hand, the channel would be too small to contain a large β-barrel such as FhuA. Another question would be, how would Omp85 adjust to the large differences in the diameters of the β-barrels of the various OMPs? Further experiments are clearly needed to really clarify possible effects of Omp85 in the stages of structure formation and β-barrel membrane protein integration. Instead of a direct involvement of Omp85 in the structure formation of OMPs, it appears more likely that Omp85 is needed for targeting of the OMPs to the outer membrane. In lack of direct experimental evidence for a role of Omp85 in membrane insertion and structure formation, the proposed translocon-like model for the action of Omp85 currently appears speculative or premature. When folding is analyzed by methods that directly report on the formation of secondary and tertiary structure in OMPs as well as on the degree of membrane insertion, folding and insertion of OMPs definitely also take place in absence of Omp85, by a concerted mechanism that is simply induced by lipid–protein interactions [62, 89, 90].

6.9
Outlook

Although the exploration of insertion and folding of β-barrel membrane proteins into membranes has made progress in recent years, our knowledge about the process is still very limited and many new questions have surfaced with the discovery of OMP targeting and/or folding machineries that exist in the periplasm, and apparently also in the outer membrane [143]. While Skp and SurA were demonstrated to improve membrane insertion and folding of OmpA *in vitro*, these chaperones had no significant effects on the insertion and folding of some other OMPs into preformed lipid bilayers. It will be interesting to note which additional chaperones will be discovered that assist the OMP assembly process in well-defined *in vitro* experiments. It will then be necessary to investigate whether these proteins are directly involved in the generation of structure in OMPs or whether they are key elements for the targeting of OMPs to the surface of the outer membrane, where OMP insertion into the phospholipid bilayer is then mediated by lipid–protein interactions. Some OMPs, e.g. OmpA, do not absolutely require folding machinery for quantitative folding *in vitro* from a urea-denatured state. However, *in vivo,* i.e. in the absence of urea, chaperones such as Skp must prevent the hy-

drophobic collapse and misfolding of OMPs, and deliver them to the outer membrane. In the case of OmpA, insertion and folding appear to be driven by the interaction of a chaperone–OmpA complex with the lipid bilayer and apparently can take place in absence of membrane-integrated proteins that act as folding machinery [68]. The folding kinetics of OmpA *in vitro* greatly depend on the properties of the lipid bilayer. These properties may be modulated by peripherally bound or by intrinsic membrane proteins. Skp, for example, is highly basic and may modulate the surface properties of the periplasmic leaflet of the outer membrane, which contains phosphatidylglycerol that is negatively charged. Future studies on the insertion and folding of β-barrel membrane proteins must therefore also include investigations on how periplasmic proteins modify the properties of the periplasmic surface of the outer membrane. In addition, more detailed information must be obtained on structure formation in OMPs. For example, it is not clear how the polar loops of the OMPs translocate across the hydrophobic core of the bilayer, and what role lipid–protein and protein–protein interactions have in this context.

References

1 G. E. Schulz. *Biochim. Biophys. Acta* **2002**, *1565*, 308–317.

2 D. Marsh, T. Páli. *Biophys. J.* **2001**, *80*, 305–312.

3 A. Arora, F. Abildgaard, J. H. Bushweller, L. K. Tamm. *Nat. Struct. Biol.* **2001**, *8*, 334–338.

4 A. Pautsch, G. E. Schulz. *J. Mol. Biol.* **2000**, *298*, 273–282.

5 J. Vogt, G. E. Schulz. *Struct. Fold. Des.* **1999**, *7*, 1301–1309.

6 C. Fernandez, K. Adeishvili, K. Wüthrich. *Proc. Natl Acad. Sci. USA* **2001**, *98*, 2358–2363.

7 C. Hilty, G. Wider, C. Fernández, K. Wüthrich. *ChemBiochem* **2004**, *5*, 467–473.

8 L. Vandeputte-Rutten, M. P. Bos, J. Tommassen, P. Gros. *J. Biol. Chem.* **2003**, *278*, 24825–24830.

9 P. M. Hwang, W. Y. Choy, E. I. Lo, L. Chen, J. D. Forman-Kay, C. R. Raetz, G. G. Privé, R. E. Bishop, L. E. Kay. *Proc. Natl Acad. Sci. USA* **2002**, *99*, 13560–13565.

10 V. E. Ahn, E. I. Lo, C. K. Engel, L. Chen, P. M. Hwang, L. E. Kay, R. E. Bishop, G. G. Privé. *EMBO J.* **2004**, *23*, 2931–2941.

11 L. Vandeputte-Rutten, R. A. Kramer, J. Kroon, N. Dekker, M. R. Egmond, P. Gros. *EMBO J.* **2001**, *20*, 5033–5039.

12 C. J. Oomen, P. Van Ulsen, P. Van Gelder, M. Feijen, J. Tommassen, P. Gros. *EMBO J.* **2004**, *23*, 1257–1266.

13 H. J. Snijder, I. Ubarretxena-Belandia, M. Blaauw, K. H. Kalk, H. M. Verheij, M. R. Egmond, N. Dekker, B. W. Dijkstra. *Nature* **1999**, *401*, 717–721.

14 B. van den Berg, P. N. Black, W. M. Clemons, Jr., T. A. Rapoport. *Science* **2004**, *304*, 1506–1509.

15 K. Zeth, K. Diederichs, W. Welte, H. Engelhardt. *Struct. Fold. Des.* **2000**, *8*, 981–992.

16 M. S. Weiss, A. Kreusch, E. Schiltz, U. Nestel, W. Welte, J. Weckesser, G. E. Schulz. *FEBS Lett.* **1991**, *280*, 379–382.

17 S. W. Cowan, R. M. Garavito, J. N. Jansonius, J. A. Jenkins, R. Karlsson, N. Konig, E. F. Pai, R. A. Pauptit, P. J. Rizkallah, J. P. Rosenbusch, et al. *Structure* **1995**, *3*, 1041–1050.

18 S. W. Cowan, T. Schirmer, G. Rummel, M. Steiert, R. Ghosh, R. A. Pauptit, J. N. Jansonius, J. P. Rosenbusch. *Nature* **1992**, *358*, 727–733.

19 T. Schirmer, T. A. Keller, Y. F. Wang, J. P. Rosenbusch. *Science* **1995**, *267*, 512–514.

20 D. Forst, W. Welte, T. Wacker, K. Diederichs. *Nat. Struct. Biol.* **1998**, *5*, 37–46.

21 S. K. Buchanan, B. S. Smith, L. Venkatramani, D. Xia, L. Esser, M. Palnitkar, R. Chakraborty, D. van der Helm, J. Deisenhofer. *Nat. Struct. Biol.* **1999**, *6*, 56–63.

22 D. P. Chimento, A. K. Mohanty, R. J. Kadner, M. C. Wiener. *Acta Crystallogr. D Biol. Crystallogr.* **2003**, *59*, 509–511.

23 G. Kurisu, S. D. Zakharov, M. V. Zhalnina, S. Bano, V. Y. Eroukova, T. I. Rokitskaya, Y. N. Antonenko, M. C. Wiener, W. A. Cramer. *Nat. Struct. Biol.* **2003**, *10*, 948–954.

24 A. D. Ferguson, E. Hofmann, J. W. Coulton, K. Diederichs, W. Welte. *Science* **1998**, *282*, 2215–2220.

25 K. P. Locher, B. Rees, R. Koebnik, A. Mitschler, L. Moulinier, J. P. Rosenbusch, D. Moras. *Cell* **1998**, *95*, 771–778.

26 S. Conlan, Y. Zhang, S. Cheley, H. Bayley. *Biochemistry* **2000**, *39*, 11845–11854.

27 V. Koronakis, A. Sharff, E. Koronakis, B. Luisi, C. Hughes. *Nature* **2000**, *405*, 914–919.

28 W. C. Wimley. *Protein Sci.* **2002**, *11*, 301–312.

29 W. C. Wimley. *Curr. Opin. Struct. Biol.* **2003**, *13*, 404–411.

30 L. Song, M. R. Hobaugh, C. Shustak, S. Cheley, H. Bayley, J. E. Gouaux. *Science* **1996**, *274*, 1859–1866.

31 A. P. Heuck, E. M. Hotze, R. K. Tweten, A. E. Johnson. *Mol. Cell.* **2000**, *6*, 1233–1242.

32 L. A. Shepard, A. P. Heuck, B. D. Hamman, J. Rossjohn, M. W. Parker, K. R. Ryan, A. E. Johnson, R. K. Tweten. *Biochemistry* **1998**, *37*, 14563–14574.

33 G. Menestrina, M. Dalla Serra, M. Comai, M. Coraiola, G. Viero, S. Werner, D. A. Colin, H. Monteil, G. Prevost. *FEBS Lett* **2003**, *552*, 54–60.

34 M. Montoya, E. Gouaux. *Biochim. Biophys. Acta.* **2003**, *1609*, 19–27.

35 A. P. Heuck, R. K. Tweten, A. E. Johnson. *Biochemistry* **2001**, *40*, 9065–9073.

36 M. Faller, M. Niederweis, G. E. Schulz. *Science* **2004**, *303*, 1189–1192.

37 M. Niederweis. *Mol. Microbiol.* **2003**, *49*, 1167–1177.

38 T. Haltia, E. Freire. *Biochim. Biophys. Acta* **1995**, *1241*, 295–322.

39 C. S. Klug, W. Su, J. Liu, P. E. Klebba, J. B. Feix. *Biochemistry* **1995**, *34*, 14230–14236.

40 J. A. Schellman. *Biopolymers* **1978**, *17*, 1235–1248.

41 C. N. Pace. *Methods Enzymol.* **1986**, *131*, 266–280.

42 F. Ahmad, C. C. Bigelow. *J. Biol. Chem.* **1982**, *257*, 12935–12938.

43 M. Yao, D. W. Bolen. *Biochemistry* **1995**, *34*, 3771–3781.

44 H. Hong, L. K. Tamm. *Proc. Natl Acad. Sci. USA* **2004**, *101*, 4065–4070.

45 D. Shortle. *Adv. Protein Chem.* **1995**, *46*, 217–247.

46 J. K. Myers, C. N. Pace, J. M. Scholtz. *Protein Sci* **1995**, *4*, 2138–2148.

47 C. N. Pace, K. E. Vanderburg. *Biochemistry* **1979**, *18*, 288–292.

48 L. Serrano, A. Horovitz, B. Avron, M. Bycroft, A. R. Fersht. *Biochemistry* **1990**, *29*, 9343–9352.

49 C. S. Klug, J. B. Feix. *Protein Sci.* **1998**, *7*, 1469–1476.

50 J. H. Kleinschmidt, M. C. Wiener, L. K. Tamm. *Protein Sci.* **1999**, *8*, 2065–2071.

51 T. Surrey, F. Jähnig. *Proc. Natl. Acad. Sci. USA* **1992**, *89*, 7457–7461.

52 T. Surrey, F. Jähnig. *J. Biol. Chem.* **1995**, *270*, 28199–28203.

53 J. A. Szule, N. L. Fuller, R. P. Rand. *Biophys. J.* **2002**, *83*, 977–984.

54 M. Bonhivers, M. Desmadril, G. S. Moeck, P. Boulanger, A. Colomer-Pallas, L. Letellier. *Biochemistry* **2001**, *40*, 2606–2613.

55 M. Schweizer, I. Hindennach, W. Garten, U. Henning. *Eur. J. Biochem.* **1978**, *82*, 211–217.

56 K. Dornmair, H. Kiefer, F. Jähnig. *J. Biol. Chem.* **1990**, *265*, 18907–18911.

57 K. S. Huang, H. Bayley, M. J. Liao, E. London, H. G. Khorana. *J. Biol. Chem.* **1981**, *256*, 3802–3809.

58 C. B. Anfinsen. *Science* **1973**, *181*, 223–230.

59 H. de Cock, J. Tommassen. *EMBO J.* **1996**, *15*, 5567–5573.

60 C. Jansen, M. Heutink, J. Tommassen, H. de Cock. *Eur. J. Biochem.* **2000**, *267*, 3792–3800.

61 N. A. Rodionova, S. A. Tatulian, T. Surrey, F. Jähnig, L. K. Tamm. *Biochemistry* **1995**, *34*, 1921–1929.

62 J. H. Kleinschmidt, L. K. Tamm. *J. Mol. Biol.* **2002**, *324*, 319–330.

63 T. Surrey, A. Schmid, F. Jähnig. *Biochemistry* **1996**, *35*, 2283–2288.

64 S. Conlan, H. Bayley. *Biochemistry* **2003**, *42*, 9453–9465.

65 S. K. Buchanan. *Curr. Opin. Struct. Biol.* **1999**, *9*, 455–461.

66 U. K. Laemmli. *Nature* **1970**, *227*, 680–685.

67 J. H. Kleinschmidt, L. K. Tamm. *Biochemistry* **1996**, *35*, 12993–13000.

68 P. V. Bulieris, S. Behrens, O. Holst, J. H. Kleinschmidt. *J. Biol. Chem.* **2003**, *278*, 9092–9099.

69 J. H. Kleinschmidt. *Cell. Mol. Life Sci.* **2003**, *60*, 1547–1558.

70 K. P. Locher, J. P. Rosenbusch. *Eur. J. Biochem.* **1997**, *247*, 770–775.

71 M. Behlau, D. J. Mills, H. Quader, W. Kühlbrandt, J. Vonck. *J. Mol. Biol.* **2001**, *305*, 71–77.

72 H. Vogel, F. Jähnig. *J. Mol. Biol.* **1986**, *190*, 191–199.

73 A. Arora, D. Rinehart, G. Szabo, L. K. Tamm. *J. Biol. Chem.* **2000**, *275*, 1594–1600.

74 R. Freudl, H. Schwarz, Y. D. Stierhof, K. Gamon, I. Hindennach, U. Henning. *J. Biol. Chem.* **1986**, *261*, 11355–11361.

75 S. J. Alvis, I. M. Williamson, J. M. East, A. G. Lee. *Biophys. J.* **2003**, *85*, 3828–3838.

76 A. S. Ladokhin. *Anal. Biochem.* **1999**, *276*, 65–71.

77 T. Markello, A. Zlotnick, J. Everett, J. Tennyson, P. W. Holloway. *Biochemistry* **1985**, *24*, 2895–2901.

78 E. J. Bolen, P. W. Holloway. *Biochemistry* **1990**, *29*, 9638–9643.

79 J. Everett, A. Zlotnick, J. Tennyson, P. W. Holloway. *J. Biol. Chem.* **1986**, *261*, 6725–6729.

80 I. M. Williamson, S. J. Alvis, J. M. East, A. G. Lee. *Biophys. J.* **2002**, *83*, 2026–2038.

81 A. S. Ladokhin, P. W. Holloway. *Biophys. J.* **1995**, *69*, 506–517.

82 A. S. Ladokhin. *Biophys. J.* **1999**, *76*, 946–955.

83 M. E. Fastenberg, H. Shogomori, X. Xu, D. A. Brown, E. London. *Biochemistry* **2003**, *42*, 12376–12390.

84 B. Piknova, D. Marsh, T. E. Thompson. *Biophys. J.* **1997**, *72*, 2660–2668.

85 F. S. Abrams, E. London. *Biochemistry* **1993**, *32*, 10826–10831.

86 M. J. Prieto, M. Castanho, A. Coutinho, A. Ortiz, F. J. Aranda, J. C. Gómez-Fernandéz. *Chem. Phys. Lipids* **1994**, *69*, 75–85.

87 A. Cruz, C. Casals, I. Plasencia, D. Marsh, J. Pérez-Gil. *Biochemistry* **1998**, *37*, 9488–9496.

88 F. S. Abrams, E. London. *Biochemistry* **1992**, *31*, 5312–5322.

89 J. H. Kleinschmidt, T. den Blaauwen, A. Driessen, L. K. Tamm. *Biochemistry* **1999**, *38*, 5006–5016.

90 J. H. Kleinschmidt, L. K. Tamm. *Biochemistry* **1999**, *38*, 4996–5005.

91 T. J. McIntosh, P. W. Holloway. *Biochemistry* **1987**, *26*, 1783–1788.

92 M. C. Wiener, S. H. White. *Biochemistry* **1991**, *30*, 6997–7008.

93 A. Chattopadhyay, E. London. *Biochemistry* **1987**, *26*, 39–45.

94 A. Pautsch, G. E. Schulz. *Nat. Struct. Biol.* **1998**, *5*, 1013–1017.

95 M. Ramakrishnan, C. L. Pocanschi, J. H. Kleinschmidt, D. Marsh. *Biochemistry* **2004**, *43*, 11630–11636.

96 D. Marsh, L. I. Horváth. *Biochim. Biophys. Acta* **1998**, *1376*, 267–296.

97 J. H. Kleinschmidt, G. L. Powell, D. Marsh. *Biochemistry* **1998**, *37*, 11579–11585.

98 J. E. Mahaney, J. Kleinschmidt, D. Marsh, D. D. Thomas. *Biophys. J.* **1992**, *63*, 1513–1522.

99 M. B. Sankaram, P. J. Brophy, D. Marsh. *Biochemistry* **1991**, *30*, 5866–5873.

100 M. Ramakrishnan, C. L. Pocanschi, J. Qu, J. H. Kleinschmidt, D. Marsh. *Biochemistry* **2005**, *44*, 3515–3523.

101 A. D. Ferguson, W. Welte, E. Hofmann, B. Lindner, O. Holst, J. W. Coulton, K. Diederichs. *Structure* **2000**, *8*, 585–592.

102 L. Steeghs, H. de Cock, E. Evers, B. Zomer, J. Tommassen, P. van der Ley. *EMBO J.* **2001**, *20*, 6937–6945.

103 P. van der Ley, L. Steeghs. *J. Endotoxin Res.* **2003**, *9*, 124–128.

104 K. Brandenburg, P. Garidel, A. B. Schromm, J. Andrä, A. Kramer, M. Egmond, A. Wiese. *Eur. Biophys. J.* **2005**, *34*, 28–41.

105 R. A. Kramer, K. Brandenburg, L. Vandeputte-Rutten, M. Werkhoven, P. Gros, N. Dekker, M. R. Egmond. *Eur. J. Biochem.* **2002**, *269*, 1746–1752.

106 T. Páli, D. Marsh. *Biophys. J.* **2001**, *80*, 2789–2797.

107 S. Grizot, S. K. Buchanan. *Mol. Microbiol.* **2004**, *51*, 1027–1037.

108 S. Arnott, S. D. Dover, A. Elliott. *J. Mol. Biol.* **1967**, *30*, 201–208.

109 A. G. Lee. *Biochim. Biophys. Acta* **2003**, *1612*, 1–40.

110 A. H. O'Keeffe, J. M. East, A. G. Lee. *Biophys. J.* **2000**, *79*, 2066–2074.

111 B. A. Lewis, D. M. Engelman. *J. Mol. Biol.* **1983**, *166*, 211–217.

112 R. Koebnik. *J. Mol. Biol.* **1999**, *285*, 1801–1810.

113 R. Koebnik. *EMBO J.* **1996**, *15*, 3529–3537.

114 R. Koebnik, L. Krämer. *J. Mol. Biol.* **1995**, *250*, 617–626.

115 H. de Cock, S. van Blokland, J. Tommassen. *J. Biol. Chem.* **1996**, *271*, 12885–12890.

116 U. Schäfer, K. Beck, M. Müller. *J. Biol. Chem.* **1999**, *274*, 24567–24574.

117 M. Müller, H. G. Koch, K. Beck, U. Schäfer. *Prog Nucleic Acid Res. Mol. Biol.* **2001**, *66*, 107–157.

118 E. H. Manting, A. J. Driessen. *Mol. Microbiol.* **2000**, *37*, 226–238.

119 P. N. Danese, T. J. Silhavy. *Annu. Rev. Genet.* **1998**, *32*, 59–94.

120 S. W. Lazar, R. Kolter. *J. Bacteriol.* **1996**, *178*, 1770–1773.

121 P. E. Rouvière, C. A. Gross. *Genes Dev.* **1996**, *10*, 3170–3182.

122 S. Behrens, R. Maier, H. de Cock, F. X. Schmid, C. A. Gross. *EMBO J.* **2001**, *20*, 285–294.

123 D. Missiakas, J. M. Betton, S. Raina. *Mol. Microbiol.* **1996**, *21*, 871–884.

124 K. Ramm, A. Plückthun. *J. Biol. Chem.* **2000**, *275*, 17106–17113.

125 H. Bothmann, A. Plückthun. *J. Biol. Chem.* **2000**, *275*, 17100–17105.

126 K. Ramm, A. Plückthun. *J. Mol. Biol.* **2001**, *310*, 485–498.

127 J. Liu, C. T. Walsh. *Proc. Natl Acad. Sci. USA* **1990**, *87*, 4028–4032.

128 N. Harms, G. Koningstein, W. Dontje, M. Müller, B. Oudega, J. Luirink, H. de Cock. *J. Biol. Chem.* **2001**, *276*, 18804–18811.

129 H. Bothmann, A. Plückthun. *Nat. Biotechnol.* **1998**, *16*, 376–380.

130 R. Chen, U. Henning. *Mol. Microbiol.* **1996**, *19*, 1287–1294.

131 H. de Cock, U. Schäfer, M. Potgeter, R. Demel, M. Müller, J. Tommassen. *Eur. J. Biochem.* **1999**, *259*, 96–103.

132 M. Schlapschy, M. K. Dommel, K. Hadian, M. Fogarasi, I. P. Korndörfer, A. Skerra. *Biol. Chem.* **2004**, *385*, 137–143.

133 T. A. Walton, M. C. Sousa. *Mol. Cell* **2004**, *15*, 367–374.

134 I. P. Korndörfer, M. K. Dommel, A. Skerra. *Nat. Struct. Mol. Biol.* **2004**, *11*, 1015–1020.

135 E. Bitto, D. B. McKay. *Structure* **2002**, *10*, 1489–1498.

136 A. E. Rizzitello, J. R. Harper, T. J. Silhavy. *J. Bacteriol.* **2001**, *183*, 6794–6800.

137 J. Werner, A. M. Augustus, R. Misra. *J. Bacteriol.* **2003**, *185*, 6540–6547.

138 R. Voulhoux, M. P. Bos, J. Geurtsen, M. Mols, J. Tommassen. *Science* **2003**, *299*, 262–265.

139 S. A. Paschen, T. Waizenegger, T. Stan, M. Preuss, M. Cyrklaff, K. Hell, D. Rapaport, W. Neupert. *Nature* **2003**, *426*, 862–866.

140 T. Waizenegger, S. J. Habib, M. Lech, D. Mokranjac, S. A. Paschen, K. Hell, W. Neupert, D. Rapaport. *EMBO Rep.* **2004**, *5*, 704–709.

141 S. Genevrois, L. Steeghs, P. Roholl, J. J. Letesson, P. van der Ley. *EMBO J.* **2003**, *22*, 1780–1789.

142 R. Voulhoux, J. Tommassen. *Res. Microbiol.* **2004**, *155*, 129–135.

143 A. E. Johnson, R. E. Jensen. *Nat. Struct. Mol. Biol.* **2004**, *11*, 113–114.

144 L. Heins, H. Mentzel, A. Schmid, R. Benz, U. K. Schmitz. *J. Biol. Chem.* **1994**, *269*, 26402–26410.

145 R. Koradi, M. Billeter, K. Wüthrich. *J. Mol. Graph.* **1996**, *14*, 51–55, 29–32.

146 N. Guex, M.C. Peitsch. *Electrophoresis* **1997**, *18*, 2714–2723.

147 T. Schwede, J. Kopp, N. Guex, M.C. Peitsch. *Nucleic Acids Res.* **2003**, *31*, 3381–3385.

148 E. Bitto, D.B. McKay. *J. Biol. Chem.* **2003**, *278*, 49316–49322.

149 W.L. Delano. *The PyMOL User's Manual.* DeLano Scientific, San Carlos, CA, **2002**.